Macromolecules
ARTICLE

Macromolecules **2009**, *42*, 4817–4828 **4817**
DOI: 10.1021/ma901055t

Barrier Capacity of Hydrophilic Polymer Brushes To Prevent Hydrophobic Interactions: Effect of Graft Density and Hydrophilicity

Yuquan Zou,[†] Nicholas A. A. Rossi,[†] Jayachandran N. Kizhakkedathu,*[,†] and Donald E. Brooks*[,†,‡]

[†]*Centre for Blood Research, Department of Pathology and Laboratory of Medicine and* [‡]*Department of Chemistry, 2350 Health Sciences Mall, University of British Columbia, Vancouver, B.C. V6T 1Z3, Canada*

Received February 13, 2009; Revised Manuscript Received May 29, 2009

ABSTRACT: The performance of biomaterials in contact with biological systems can be greatly affected by hydrophobic interactions at the interface between the biomaterial surface and surrounding biomolecules. Polymer brushes can function as a protective layer, preventing such interfacial hydrophobic interactions. In this paper, a systematic study of the barrier properties of a hydrophilic polymer brush is made by investigating the influence of graft density and its chemical nature (hydrophilicity/hydrophobicity) on hydrophobic interactions with the surface. To achieve this, a series of novel thermoresponsive poly-*N*-[(2,2-dimethyl-1,3-dioxolane)methyl]acrylamide (PDMDOMA) polymer brushes were grown from silicon wafers via surface-initiated atom transfer radical polymerization. Without changing graft density or degree of polymerization, the hydrophilicity of the PDMDOMA brushes was manipulated by partial or complete hydrolysis of the pendent dioxolane moieties. A lower critical solution temperature (LCST) was observed at 22−24 °C, below which the PDMDOMA brush was found to be in a hydrated state (amphiphilic), while at temperatures above the LCST, the PDMDOMA brush formed a collapsed, more hydrophobic structure. A physical method was developed to analyze the ability of these brushes to act as a barrier against hydrophobic interactions based on AFM force−distance measurements. The adhesive forces between the Si_3N_4 tip and the silicon wafer surface upon (a) modification with ATRP initiator, (b) grafting of PDMDOMA brushes, and (c) partial and complete hydrolysis of PDMDOMA were investigated. Hydrophobic interactions decreased after each modification, while graft density and the degree of hydrolysis increased the barrier function of the surface layer. In particular, when graft density was above 0.22 chains/nm^2, the barrier capacity completely counteracted the hydrophobic interactions, as evidenced from the disappearance of the adhesive force in AFM measurements. Further studies revealed that the barrier property as assessed by AFM correlated well with the wettability of the surfaces.

1. Introduction

Biocompatibility is the primary concern for the development of many novel biomaterials.[1] It has been shown that when a biomaterial comes into contact with a biofluid, a series of events take place at the interface. In the case of blood, plasma protein adsorption is usually observed, followed by platelet adhesion, thrombus formation, and inflamation.[2] These responses are particularly pronounced for hydrophobic materials such as poly(vinyl chloride) (PVC) and poly(methyl methacrylate) (PMMA), all of which have found application in various biomedical settings.[3−5] Although many different factors can account for these events, hydrophobic interactions (F_H) have been identified as one of the most important driving forces. For instance, it is well-known that hydrophobic interactions between proteins and polymers in solution or on surfaces can lead to protein−polymer binding.[6−10] Therefore, significant efforts have been devoted to minimizing the effects of F_H through surface modifications.[11−17] Unfortunately, no truly biocompatible surface has yet to be realized using such methods, while little is known about the true effect certain modifications have on F_H.[2]

One approach to minimizing surface−protein interactions has centered on the growth of a layer of hydrophilic polymer brushes from the surfaces of relatively hydrophobic materials. To date, many different polymer brush systems have been developed in attempts to generate more biocompatible surfaces, including poly(ethylene glycol), phosphorylcholine-based polymers (PC polymers), hyperbranched polyglycerol (HPG), polyacrylamide, poly(sulfobetaine methacrylate) (polySBMA), and poly(carboxybetaine methacrylate) (polyCBMA).[18−28] In general, the goal for the grafted polymer brush is to function as a barrier layer to minimize the interactions between the underlying surface and components such as proteins present in the biofluid. When the barrier capacity of a polymer brush is sufficiently high, interaction between the biofluid and the underlying layer can, in principle, be totally shielded.

Hydrophobic interactions are thermodynamic in nature, deriving from the gain in entropy that occurs when the water structure that forms around hydrophobic groups is reduced by the associating hydrophobic species.[29] This results in a smaller surface area being exposed to the aqueous medium with an attendant reduction in structured water. A measure of the magnitude of the free energy change associated with hydrophobic association can be obtained by careful calorimetric measurements, which is the classical approach to assessing the hydrophobic effect.[30] In principle, barrier properties such as the ones addressed in this paper can be assessed by such calorimetric measurements. However, to assess hydrophobic associations of macromolecules with surfaces, large surface areas and sensitive calorimeters are required, limiting the applicability of this technique. Recently, Geisler et al. employed single-molecule force

*To whom correspondence should be addressed: e-mail jay@pathology.ubc.ca (J.N.K.) or don.brooks@ubc.ca (D.E.B.); Tel +1-604-822-7085; Fax +1-604-822-7742.

Published on Web 06/12/2009

microscopy to study the hydrophobic effect on protein adsorption onto a solid substrate, which provided an opportunity to studying the hydrophobic interactions.[31] In the present work we utilize force−distance measurements carried out in water with a Si_3N_4 atomic force microscope (AFM) tip approaching and retracting from a modified silicon wafer surface. When the wafer is derivatized with an electrically neutral hydrophobic ATRP initiator, the force measurements show a strong, short-range attraction between the tip and the surface. This attraction, which is due to a hydrophobic interaction with the surface, is absent when the wafer is not derivatized with the initiator.

Growth of hydrophilic brushes from the initiators reduces the net attractive force, the magnitude of which provides a quantitative measure of the effect of the brush barrier on the interaction. Varying the properties of the brush and repeating the force−distance measurements provides a facile method for assessing the barrier properties of the polymer layer. Here, we report the synthesis of a novel class of polymer brushes whose properties can be readily varied without changing the graft density or chain length of the grafted chains. The barrier capacity of these brushes was mediated by varying (1) the hydrophilicity/hydrophobicity of the brushes by chemically cleaving the monomer side chains and (2) the graft density of the brushes. Through a systematic analysis of the AFM interaction forces, we have investigated the effect of different brush properties in preventing hydrophobic interactions in water. Furthermore, a correlation between the barrier property and surface wettability has also been established.

2. Experimental Section

2.1. Materials and Methods. 2,2-Dimethyl-1,3-dioxolane-4-methanamine (Aldrich, 97%), methyl 2-chloropropionate (Aldrich, 99%), 1,1,4,7,10,10-hexamethyltriethylenetetramine (HMTETA, Aldrich, 97%), CuCl (Aldrich, 99 + %), and $CuCl_2$ (Aldrich, 99.99%) were used as supplied. All other commercial reagents were purchased from Aldrich of the highest purity and used without further purification. Silicon wafers were purchased from University Wafer (Boston, MA) with one side polished. Water was purified using a Milli-Q Plus water purification system (Millipore Corp., Bedford, MA) and was used in all experiments.

2.2. Instrumentation. Static water contact angles were determined by dripping a water droplet of 2 μL on a silicon wafer before a picture of the droplet was taken using a digital camera (Retiga 1300, Q-imaging Co.). Water contact angle was analyzed with Northern Eclipse software. Five different sites were tested for each sample, and the average value is reported. Film thicknesses of the grafted poly-*N*-[(2,2-dimethyl-1,3-dioxolane) methyl]acrylamide (PDMDOMA) brushes were measured in air by ellipsometry. The variable-angle spectroscopic ellipsometry (VASE) spectra were collected on an M-2000 V spectroscopic ellipsometer (J.A. Woollam Co. Inc., Lincoln, NE) at 45°, 55°, and 65°, at wavelengths from 370 to 1000 nm with an M-2000 50 W quartz tungsten halogen light source. The VASE spectra were then fitted with a multilayer model utilizing WVASE32 analysis software, based on the optical properties of a generalized Cauchy layer to obtain the "dry" thickness of the PDMDOMA brush layer. X-ray photoelectron spectroscopy (XPS) was performed using a Leybold LH Max 200 surface analysis system (Leybold, Cologne, Germany) equipped with a Mg Kα source at a power of 200 W. Elements were identified from survey spectra. High-resolution spectra were also collected at 48 eV pass energy. Prior to XPS analysis, all samples were thoroughly dried in vacuum. Attenuated total reflectance Fourier transform infrared (ATR-FTIR) spectra were recorded using a Thermo-Nicolet Nexus FT-IR spectrometer with a MCT/A liquid nitrogen cooled detector, KBr beamsplitter, and MKII Golden Gate single reflection attenuated total reflectance accessory (Specac Inc.). Spectra were recorded at 4 cm^{-1} resolution, and 100 scans were collected.

Absolute molecular weights of the "free" polymers were determined by gel permeation chromatography (GPC) on a Waters 2690 separation module fitted with a DAWN EOS multiangle laser light scattering (MALLS) detector from Wyatt Technology Corp. with 18 detectors placed at different angles (laser wavelength $\lambda = 690$ nm) and a refractive index detector from Viscotek Corp. operated at $\lambda = 620$ nm.

For PDMDOMA, 0.05 M LiBr/DMF solution was used as the mobile phase at a flow rate of 0.8 mL/min. Aliquots of 200 μL of the polymer solution were injected through Styragel columns (Waters) at 22 °C (guard column, Styragel HR1, elution range 100−5000 Da, and HR 5E mixed bed column, elution range 2000−4×10^6 Da). The dn/dc value for PDMDOMA in the mobile phase was determined at $\lambda = 620$ nm as 0.05 mL/g (determined online using the RI detector response from a number of different concentrations of pure polymer) and was used for calculating the molecular weights. For partial or 100% cleaved PDMDOMA, a 0.1 M $NaNO_3$ aqueous solution was used as the mobile phase at a flow rate of 0.8 mL/min. Aliquots of 200 μL of the polymer solution were injected through the Ultrahydrogel columns at 22 °C (guard column, Ultrahydrogel linear with bead size 6−13 um, elution range 10^3−7×10^6 Da, and Ultrahydrogel 120 with bead size 6 um, elution range 150−5×10^3 Da connected in series; from Waters). The dn/dc value for 100% cleaved PDMDOMA in 0.1 M $NaNO_3$ was determined at $\lambda = 620$ nm as 0.162 mL/g and was used for molecular weight calculations.

In the current study, brush molecular weight characteristics were estimated from the solution polymer formed along with the grafted chains, an approximation that is widely used.[32] We supported this assumption by estimating the molecular weight of the grafted S4-PDMDOMA polymer via AFM according to our previously reported pull-off method.[33] The number-average molecular weights obtained by the two methods were comparable (19 300 Da by AFM and 20 800 Da from solution GPC; Figure 4S, Supporting Information). Therefore, the molecular weight characteristics obtained in this study should reflect the properties of surface polymers reasonably well.

2.3. Preparation of ATRP Initiator-Deposited Silicon Wafers and Surface-Initiated Atom Transfer Radical Polymerization (SI-ATRP). A trichlorosilane-functionalized surface was prepared according to the literature with small modifications.[34] Briefly, a silicon wafer was first treated using "piranha" solution (30/70 30% aqueous hydrogen peroxide solution/sulfuric acid) at 90 °C for 1 h. *It should be noted that piranha solution is extremely reactive and as such should be handled with great care.* Ω-Undecylenyl alcohol was esterified with an equimolar amount of 2-chloropropionyl chloride and then hydrosilated using trichlorosilane and Karstedt's catalyst. The obtained attachable initiator, 11-(2-chloro)propionyloxyundecenyltrichlorosilane, was deposited onto freshly cleaned wafers by adding 10 μL of initiator into a vial containing 10 mL of anhydrous toluene and silicon wafer. The typical thickness of a dry initiator layer was 2 nm after 16 h of incubation at ambient temperature. The successful deposition of the ATRP initiator layer was verified by XPS.

All polymerizations were carried out in a glovebox filled with argon at room temperature. Synthesis of DMDOMA monomer and SI-ATRP of DMDOMA[35,36] followed the conditions reported earlier by our group. For a typical reaction, the initiator-deposited silicon wafer was cut into 1 cm × 1 cm pieces and placed into a 20 mL glass vial. A two-neck round-bottom flask was loaded with CuCl (15 mg, 0.15 mM), $CuCl_2$ (2 mg, 0.015 mM), HMTETA (80 mg, 0.30 mM), and DMDOMA (1 g, 5 mM) with 1 mL of DMF as the solvent. The solution was sealed and cycled three times between argon and vacuum to remove oxygen before addition to the vial containing the silicon wafer. Soluble initiator methyl 2-chloropropionate (MCP, 5 μL) was also added. The polymerization proceeded at ambient temperature for a predetermined time, after which silicon wafer

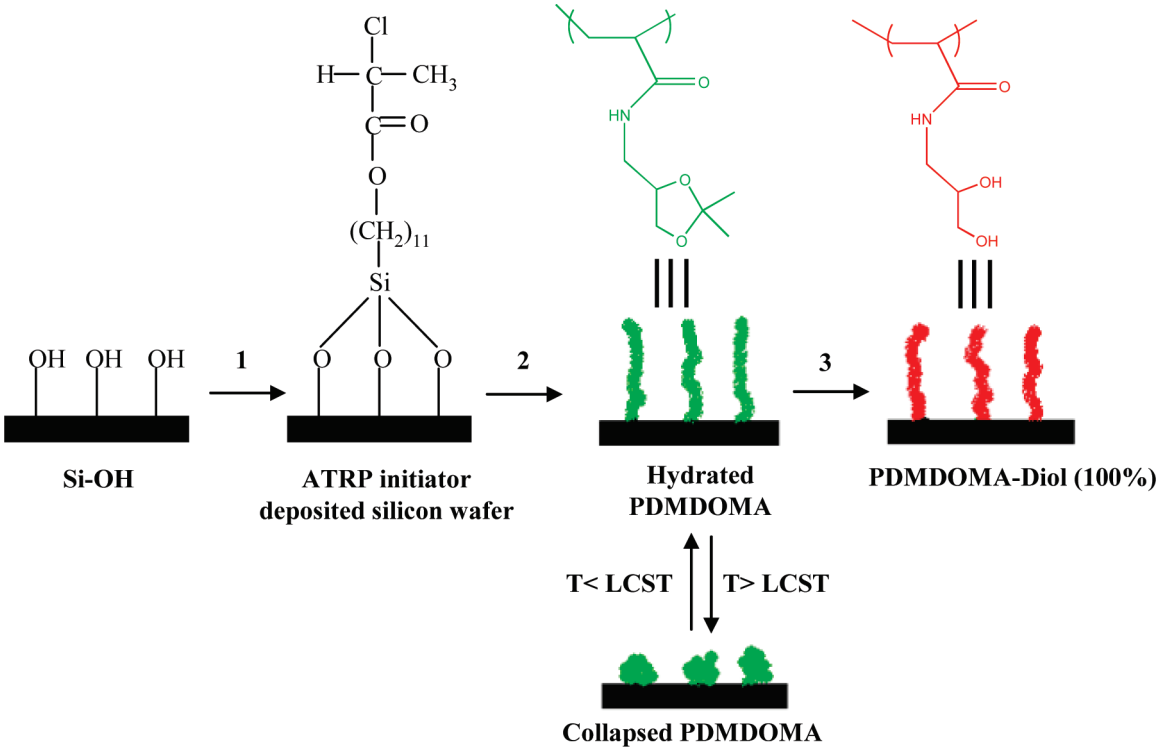

Figure 1. Preparation of PDMDOMA-grafted silicon wafer via surface-initiated atom transfer radical polymerization (SI-ATRP): (1) deposition of self-assembled ATRP initiator, 11-(2-chloro)propionyloxyundecenyltrichlorosilane; (2) SI-ATRP of DMDOMA from wafer surface; (3) acidic hydrolysis of PDMDOMA brushes to obtain PDMDOMA-diol (100%) brush.

was removed, sonicated, and thoroughly rinsed with DMF and water to remove physically adsorbed polymers. The wafer was then stored in water until use. Free polymer from the polymerization solution was purified by dialysis against water for 3 days and lyophilized. The obtained PDMDOMA was completely hydrolyzed using 10% acetic acid solution at 45 °C for 2 h, dialyzed against water for 3 days, and analyzed by GPC-MALLS. The chemical structure of PDMDOMA on the silicon wafer was probed using ATR-FTIR.

2.4. Synthesis of PDMDOMA-diol (28% and 100%) Polymer Brushes. A Si/SiO_2/PDMDOMA polymer brush was prepared as described above. To prepare PDMDOMA-diol (100%), the wafer with a polymer brush was placed into a 20 mL glass vial before being filled with 10% acetic acid solution. The reaction proceeded at 45 °C for 2 h, and then the wafer was isolated and rinsed thoroughly with water. PDMDOMA-diol (28%) was prepared by following a similar procedure; in this case, the reaction time was only 30 min. To prepare PDMDOMA-diol brushes with different diol content, different reaction times (15, 45, 60, and 90 min) were used.

As a control, free (soluble) PDMDOMA was hydrolyzed under similar conditions. The degree of dioxolane cleavage and LCST of hydrolyzed PDMDOMA was characterized by ^1H NMR (Figure 3S, Supporting Information) and UV−vis measurements.

2.5. AFM. Atomic force microscopy measurements were performed on a multimode, Nanoscope IIIa controller (Digital Instruments, Santa Barbara, CA) equipped with an atomic head of 100×100 μm^2 scan range. AFM measurements were performed in air or underwater in contact mode using a commercially manufactured V-shaped silicon nitride (Si_3N_4) cantilever with gold on the back for laser beam reflection (Veeco, NP-S20). The spring constant of the AFM cantilever was measured using the thermal equipartition theorem.[37,38] Force measurements were performed on this instrument using a fluid cell modified to allow temperature adjustment and measurement. The experiments were performed under water in force mode. On tip approach the onset of the region of constant compliance was used to determine the zero distance, and on retraction the region in which force was unchanged was used to determine the zero force. The rate of tip−sample approach or retraction was typically 1 μm/s but ranged between 0.05 and 5 μm/s. The dependence of the maximum adhesive force on tip velocity was evaluated by measuring adhesive force at different approach and retraction speeds (50 nm/s, 1 μm/s, and 5 μm/s; Supporting Information, Figure 1S). No significant dependences were observed.

The raw AFM force data (cantilever deflection vs displacement data) were converted into force vs separation following the principle of Ducker et al. by using custom Matlab v.5.3 (Math Works, Natick, MA) software.[39] The software converts the cantilever deflection vs linear voltage displacement transformer signal into restoring force vs tip−substrate separation using user input trigger and spring constant values. The equilibrium thickness L_e of the brushes was determined as the critical distance from the substrate surface beyond which no repulsive force was detectable.

3. Results and Discussion

3.1. SI-ATRP of DMDOMA and Derivatization of PDMDOMA Brushes. Figure 1 illustrates the synthetic procedure for the PDMDOMA brush and its diol derivative. The detailed discussion of the synthesis of PDMDOMA brushes will be presented in a forthcoming paper.[36] Briefly, a self-assembled ATRP initiator layer was deposited onto silicon wafer according to the literature method.[34] DMDOMA was polymerized from wafers via SI-ATRP in DMF using a copper-based catalytic system according to a procedure outlined previously by our group.[35] The characteristics of the PDMDOMA polymer brushes are shown in Table 1. Molecular weights of the brushes were estimated from molecular weights of the corresponding free polymers formed along with grafted chains in the reaction medium.

Table 1. SI-ATRP of DMDOMA from Silicon Wafer[a]

samples	reaction time (h)	$M_{n,SEC}$ of "free" polymer[b] (Da)	$M_w/M_{n,SEC}$ of free polymer	h[c] (nm)	graft density[d] (chains/nm^2)	L_e[e] (nm)	D/R_g[f]
S1	4	18 600	1.16	1.1 ± 0.1	0.044	ND	1.6
S1-diol (100%)				1.3 ± 0.1		ND	
S2	6	19 100	1.20	2.4 ± 0.1	0.089	ND	1.1
S2-diol (100%)				2.4 ± 0.1		ND	
S3	8	18 280	1.21	3.1 ± 0.1	0.12	14	0.96
S3-diol (100%)				3.0 ± 0.2		16	
S4	12	20 800	1.18	6.3 ± 0.3	0.22	26	0.71
S4-diol (100%)				6.7 ± 0.2		29	
S5	24	20 600	1.18	8.9 ± 0.5	0.31	34	0.51
S5-diol (100%)				8.7 ± 0.3		32	

[a] Experimental conditions: DMDOMA:DMF = 1:2 (w/v), [CuCl]:[$CuCl_2$]:[HMTETA] = 1:0.1:2; reaction temperature=25 °C. [b] GPC was obtained by running PDMDOMA-diol (100%) in 0.1 M $NaNO_3$/aqueous solution. [c] h: dry thickness of PDMDOMA brush measured by ellipsometry. [d] Graft density was calculated by the equation $\sigma = \rho h N_A/M_n$. ρ of PDMDOMA was 1.2 g/cm^3, which is typical for polyacrylamides. [e] L_e: equilibrium thickness of PDMDOMA brush measured in hydrated state by AFM; T = 23 °C. Standard deviation of L_e test was about 10% of the mean value. [f] D denotes the average distance between grafting points; R_g denotes radius of gyration of polymer. When $D/R_g > 2$, grafted polymer belongs to the mushroom regime; when $D/R_g < 2$, grafted polymer forms a polymer brush.[53]

The graft densities of samples S1 to S5 gradually increased while molecular weights and polydispersities were comparable, ensuring an unambiguous comparison of the effects of graft density. The graft density was calculated by h, the dry polymer thickness determined by ellipsometry utilizing the following equation: $\sigma = h\rho N_A/M_n$, where ρ is the density of PDMDOMA (1.20 g/cm^3), N_A is Avogardro's number, and M_n is the number-average molecular weight.[40] The relatively low molecular weight distribution implied a quite uniform PDMDOMA brush. The dry thicknesses of S1 to S4 were characterized by ellipsometry, and the equilibrium thickness of hydrated S3 to S5 in water was estimated by AFM. ATR-FTIR spectra showed characteristic amide peaks (1640 cm^{-1}). The intensity of the peaks increased with increase in thickness of the brush (data not shown). PDMDOMA brushes (S1 to S5) were hydrolyzed by 10% acetic acid at 45 °C for 2 h to yield a complete and quantitative conversion to PDMDOMA-diol (100%) brush. The mild hydrolytic conditions ensured that only the dioxolane groups, and not the ester linkages (between the chains and surface), were cleaved. The dry thicknesses of S1 to S5-diol (100%) were comparable to their PDMDOMA counterparts, verifying the selective hydrolysis of the dioxolane side group (Table 1).

3.2. Controlling Hydrophilicity and Graft Density of PDMDOMA Brushes. For this study, it was crucial to generate a series of PDMDOMA brushes with different graft densities and hydrophilicities. A recurring problem regarding the synthesis and comparison of polymers, and in particular polymer brushes, has been the comparison of properties of polymers synthesized using different monomers or reaction conditions. Ideally, when one parameter is tuned, the other should remain constant so that observed differences in brush effects can be unambiguously interpreted. In this work a gradual increase in graft density was achieved by controlling polymerization time, while maintaining almost constant molecular weight and polydispersity (Table 1, S1 to S5).

To achieve a scale of hydrophilicity, two special properties of the PDMDOMA brushes were utilized. In agreement with our recent published work on soluble PDMDOMA in water,[35] PDMDOMA brushes underwent a phase transition at ~23 °C in water. When the temperature was kept below the LCST, the PDMDOMA chains existed in their hydrated state and were relatively hydrophilic. When the temperature was raised above the LCST, the PDMDOMA chains became more hydrophobic and collapsed. This property has been observed for several other thermoresponsive polymer brushes, including poly(*N*-isopropylacrylamide) (PNIPAM) brushes.[41−43] In addition, the hydrophilicity of PDMDOMA was increased by hydrolysis of the acid labile dioxolane side groups due to the generation of 1,2-diol moieties on the polymer chains (Figure 1). In a previous study we have shown that the hydrophilicity of the PDMDOMA-diol can be controlled by tuning the ratio of diols to dioxolanes present in a soluble polymer.[35] By combining these two properties, four different types of PDMDOMA or PDMDOMA-diol brushes were generated without changing the graft density and degree of polymerization and are comprised of the following: (1) the collapsed PDMDOMA brush representing the hydrophobic state (temperature $T >$ LCST), (2) the hydrated PDMDOMA brush representing the amphiphilic state ($T <$ LCST), and (3) the PDMDOMA-diol (28%) and (4) the PDMDOMA-diol (100%) representing variations of the hydrophilic state.

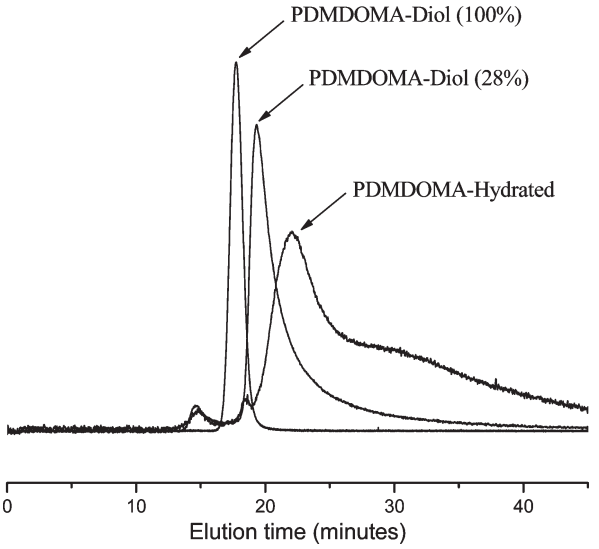

Figure 2. GPC-MALLS profiles of PDMDOMA-hydrated, PDMDOMA-diol (28%), and PDMDOMA-diol (100%, M_n = 5200 Da, M_w/M_n=1.12). GPC was run in 0.1 M $NaNO_3$ at 21 °C with 1 mg/mL of polymer concentration.

A qualitative comparison of the hydrophilicities of these four polymer brush systems was obtained from aqueous GPC elution profiles of the corresponding soluble polymers made under identical conditions using an Ultrahydrogel column (Waters) (Figure 2). It is expected that an amphiphilic or hydrophobic polymer should have more column adsorption than a highly hydrophilic polymer

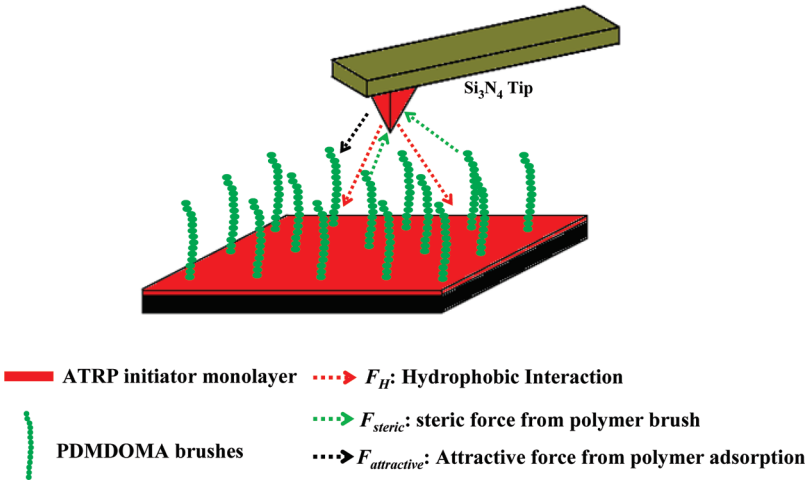

Figure 3. Illustration of three different interactions between the AFM tip and the Si/SiO_2/initiator/PDMDOMA surface. (1) F_H: hydrophobic interaction between the Si_3N_4 tip and the self-assembled ATRP initiator layer; (2) F_{steric}: steric interaction between the Si_3N_4 tip and the PDMDOMA brushes; (3) $F_{attractive}$: attractive force between the PDMDOMA brushes and the Si_3N_4 tip.

under the conditions studied. Three polymers, PDMDOMA, PDMDOMA-diol (28%), and PDMDOMA-diol (100%), were injected. The collapsed PDMDOMA was precipitated in eluent solution (0.1 M $NaNO_3$), suggesting a relatively high hydrophobicity under those conditions and as such could not be analyzed via aqueous GPC. Although PDMDOMA was soluble in water at low temperature ($T <$ LCST), it adsorbed significantly to the column, demonstrating its amphiphilicity (severe tailing of the peak). The partially cleaved PDMDOMA-diol (28%) showed slight column adsorption and PDMDOMA-diol (100%) did not show any column adsorption, indicating a higher degree of hydrophilicity. We assumed that the characteristics of the soluble polymers will hold true for the surface grafted chains. More information on the hydrophilicity of the brushes was obtained from the water contact angle measurements and is discussed in section 3.6. Thus, based on the results, the hydrophilicities of PDMDOMA based brushes increased in the order

collapsed PDMDOMA < hydrated PDMDOMA < PDMDOMA-diol (28%) < PDMDOMA-diol (100%)

3.3. Interactions between the AFM Tip and Surfaces: A Model for Surface Analysis. To study the barrier effect of a polymer brush inhibiting a hydrophobic interaction, a system containing two basic elements was used to analyze interactions between the surface and the hydrophobic AFM tip: (1) a strong hydrophobic interaction (between the tip and the C_{11} alkyl chain on the initiator) and (2) a polymer brush functioning as barrier layer with variable graft density and hydrophilicity.

As shown in Figure 3, three different interactions were considered to be in existence at the Si/SiO_2/initiator/PDMDOMA brush interface, including (1) a hydrophobic interaction of the Si_3N_4 tip (a hydrophobic material) and the underlying ATRP initiator layer (F_H), (2) a steric repulsion from the polymer brush (F_{steric}), and (3) an attractive interaction between the Si_3N_4 tip and the polymer brush caused by adsorption of polymer to the tip ($F_{attractive}$).[44] Other interactions such as electrostatic interactions were not considered in the current study due to the neutral nature of the surface and PDMDOMA brushes. F_H, a strong hydrophobic interaction between the tip and the hydrophobically modified silicon surface, represents the first element of the model. The evolution of this interaction after the grafting of different polymer chains on the surface was used to evaluate the overall barrier capacity of the brushes. The second interaction, F_{steric}, involves a unique property of tethered polymers. In good solvents, a polymer brush usually shows a repulsive force when interacting with Si_3N_4 tip.[44,46,47] Previous studies by our group and others have shown that the hydrophilic brushes such as poly(*N,N*-dimethylacrylamide) (PDMA) exhibited steric effects when interacting with the Si_3N_4 tip in water, leading to an exponentially decaying repulsive force during approach or retraction processes.[44] Similar phenomena have also been observed for hydrophobic polymer brushes in organic solvents.[46,47] F_H and F_{steric} are two opposing interactions that tend to counteract each other. In contrast, the third interaction, $F_{attractive}$, has rarely been addressed. However, we recently showed with PNIPAm brushes that this force is likely due to adsorption of polymer chains to the tip surface since the distribution of retraction distances at which the force disappears correlates closely with the molecular length distribution of the brush polymers.[33,48] The similar observation was also reported by Sonnenberg et al.[45] In the current study, $F_{attractive}$ needs to be considered due to the amphiphilic nature of some of the brushes studied here. GPC profiles shown in Figure 2 indicate that hydrated PDMDOMA and PDMDOMA-diol (28%) have some hydrophobic character, which presumably leads to attractive interactions between the polymer and the hydrophobic AFM tip in water. Hence, a combination of these three interactions needs to be addressed when determining the barrier capacity of these polymer brushes.

3.4. Hydrophobic Interaction between the Si_3N_4 Tip and the ATRP Initiator-Deposited Wafer Surface (F_H). Figure 4A shows representative force curves (both approach and retraction) between the Si_3N_4 tip and the ATRP initiator-deposited wafer surface in water. The nature of the force curves indicates the existence of strong adhesive forces. In the approach curve, the jump-to-contact (JTC) of the cantilever was observed when the tip came close to the surface at D=6 nm. During retraction, or pull-off, a much stronger adhesive force was observed. This is attributed to the short-range adhesive force caused by strong hydrophobic interactions and is typical for interactions between the Si_3N_4 tip and a hydrophobic surface.[49,50] Statistical studies indicated a

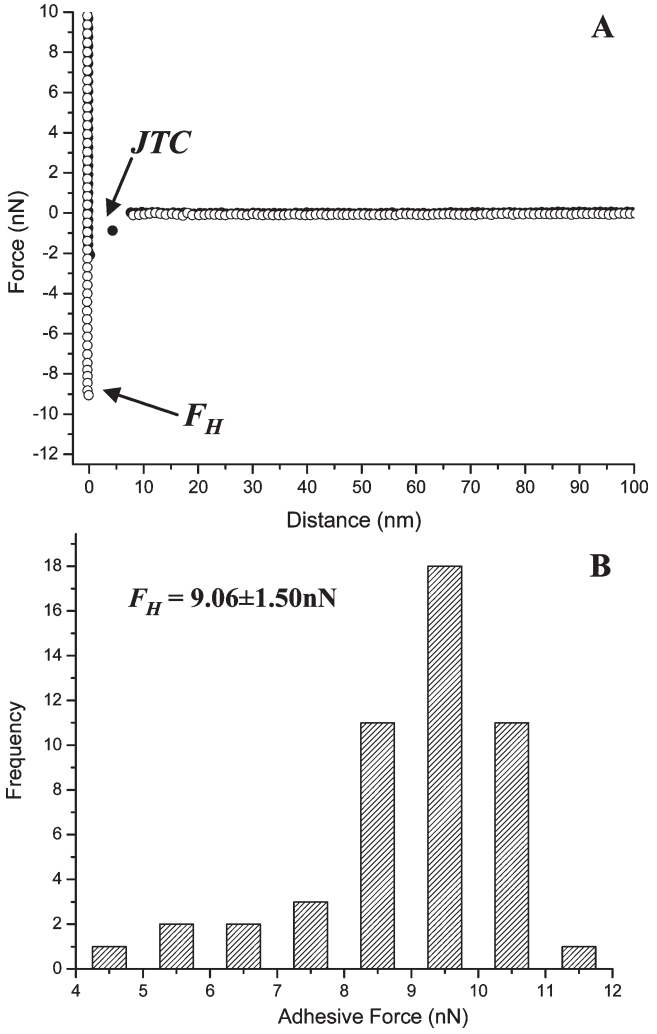

Figure 4. (A) Hydrophobic−hydrophobic interaction (F_H) between ATRP initiator-deposited silicon wafer and Si_3N_4 tip. Filled circle: approach; open circle: retract. (B) Probability distribution histograms for the maximum adhesive force during retraction.

magnitude of 9.06 ± 1.5 nN adhesive force, taken from an average of 50 spots. This was significantly higher than the JTC force encountered upon approach (2.6 ± 1.1 nN). Therefore, to obtain a better comparison between the different samples, the maximum adhesive force during retraction was chosen as the reference to evaluate the barrier capacity of different PDMDOMA/PDMDOMA-diol brushes: the higher the barrier capacity, the lower the reference force. Since there is no polymer present, only F_H (9.06 ± 1.50 nN) was observed for a wafer surface modified with ATRP initiators. It was noted that 6 out of 50 profiles showed a very weak rupture force (ca. 0.1 nN) at 60−70 nm (Supporting Information, Figure 2S). Since no polymer was grafted from these initiator-deposited surfaces, such a long rupture distance is most likely due to contamination from an unknown source, not uncommon for hydrophobic surfaces. However, the small force has little influence on the statistical analysis of F_H.

3.5. Barrier Capacity of PDMDOMA/PDMDOMA-diol Brushes. To have an unambiguous comparison of the barrier capacity of polymer brushes with different hydrophilicities, the molecular weights and graft densities of the polymer brushes must be comparable. It is known that a change in molecular weight and graft density of a polymer brush can influence surface interaction significantly.[20,21,24] In the current study, four types of polymer brushes with varying degrees of hydrophilicity were generated from a single PDMDOMA brush by altering thermoresponsiveness and the quantitative hydrolysis of the dioxolane side groups so no differences in graft density or significant differences in molecular weight were present. The brushes used in the current study have properties that represent a significant cross section of the neutral polymer brushes reported previously in the literature. Collapsed PDMDOMA brushes can be viewed as representing hydrophobic brushes in poor solvents, while hydrated PDMDOMA and PDMDOMA-diol (28%, LCST ~ 49 °C) represent amphiphilic polymers with varying hydrophobicity. PDMDOMA-diol (100%) represents a highly hydrophilic brush in good solvents. Thus, results obtained from this design can be considered representative of most neutral brush systems.

3.5.1. Effect of Graft Density on the Barrier Capacity of PDMDOMA-diol (100%). To simplify the study, PDMDOMA-diol (100%; S1-diol to S5-diol) brushes with graft densities ranging from 0.044 to 0.31 chains/nm^2 (Table 1) were initially investigated in order to study the effect of graft density on barrier capacity. Figure 5 shows the AFM force measurements and probability distribution histograms for the maximum adhesive force for S1-, S3-, and S4-diol (100%) brushes. From GPC, contact angle measurements and LCST data, it is clear that the PDMDOMA-diol (100%) brushes are very hydrophilic. Nonetheless, unlike what we observed for other highly hydrophilic polymers such as PDMA,[44] we found evidence of weak attractive forces between the tip and brush on retraction, provided the brush was not too dense (Figure 5A,B). The evidence for this statement is found in the width of the attractive portion of the retraction curve in which a significant attraction is evidenced over a distance of ~25−30 nm from the surface. This type of force−distance behavior can only be due to polymer effects as the hydrophobic attraction is present over much shorter distances, as seen in Figure 4A. We believe the attractive force is due to the weak adsorption of polymer chains to the tip that are present until the tip retracts beyond their maximum extension. We have previously used this model to estimate the length and hence molecular weight distribution of polymers in a brush and shown that the molecular weight distribution thus obtained agrees with GPC results,[33] so we have considerable confidence in this explanation.

The effect of the polymer adsorption to the tip is not seen as the brush density is increased, however (Figure 5C). Brush S1, in which the average polymer separation is approaching two radii of gyration (R_g) (Table 1), must contain fairly relaxed chains with considerable free volume since they are not far into the brush regime in which the chains interact and are repelled by their nearest neighbors (interchain separation $< 2R_g$). This allows the chains to rearrange and adsorb to the tip once it is near the surface. The chain density is sufficiently low that almost no repulsion is recorded by the tip on approach, and a weak JTC is observed within ~5 nm of the surface. Figure 5B shows the approach curve or S3 (0.12 chains/nm^2) exhibits a repulsive force instead of a JTC, although the retraction curve still shows the presence of a short-range hydrophobic attraction. At this density the chains more strongly interact as they are separated by ~R_g. This crowding causes the chains to extend away from the surface, and the extended chains exert a weak steric repulsion on the tip as it approaches closer than ~10 nm from the surface. The density is such that again some weak adsorption to the tip occurs, and on retraction the resulting attractive force is again felt out to about 25 nm (arrow a), again consistent with the maximum polymer extension. It is noted

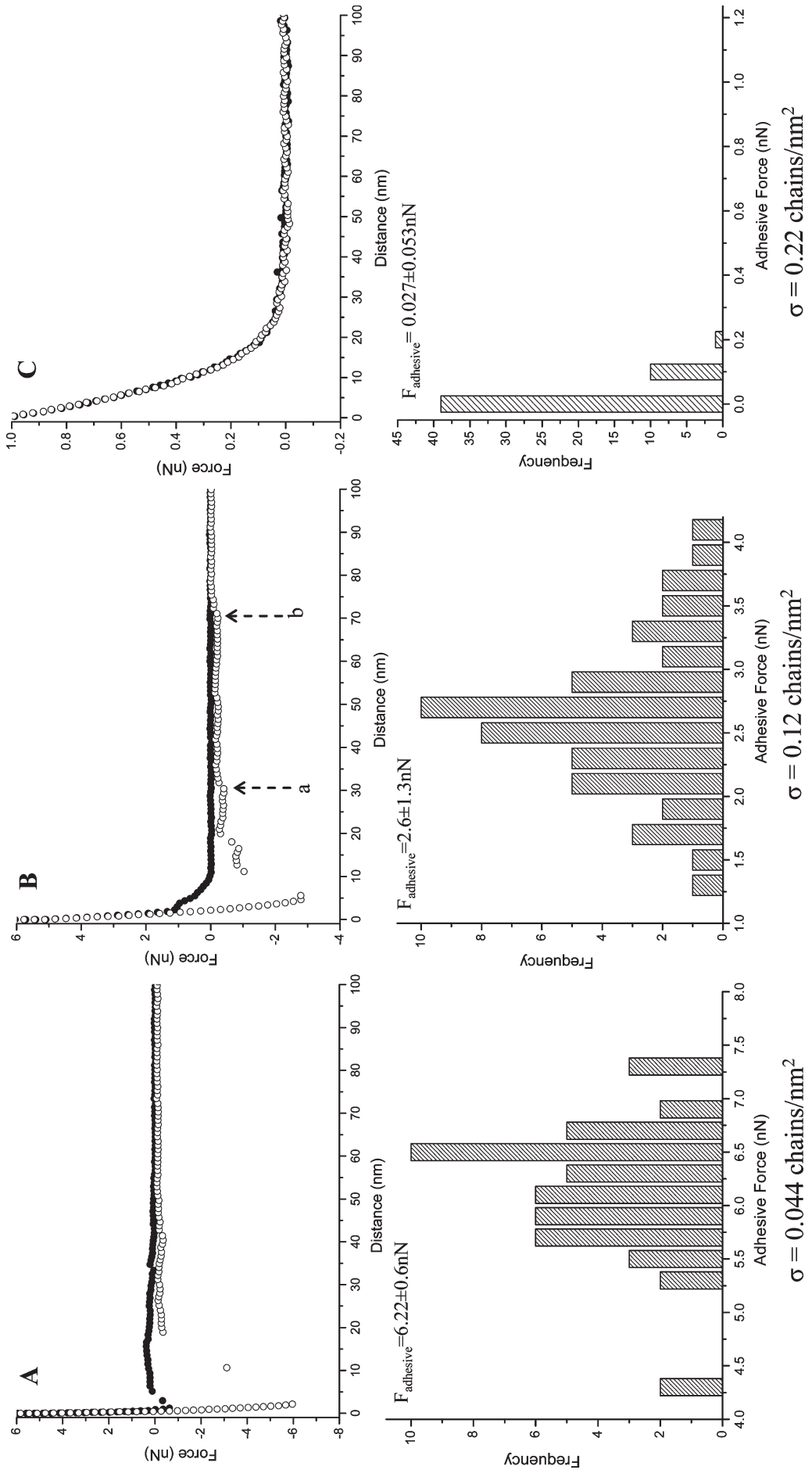

Figure 5. Representative force curves (filled circle: approach; open circle: retract) and probability distribution histograms for the maximum adhesive force during retraction: (A) S1, $\sigma = 0.044$ chains/nm^2; (B) S3, $\sigma = 0.12$ chains/nm^2; (C) S4, $\sigma = 0.22$ chains/nm^2. $T = 23$ °C. Arrows a and b in (B) represent the detachment of short polymer chains and occasional longer chains, respectively.

that 9 out of 50 measurements show an additional rupture force (indicated by arrow b) at separations ranging from 50 to 70 nm, significantly higher than the average contour length (~26 nm). The long rupture distance may be due to the detachment of occasional longer surface polymer chains, consistent with a low degree of heterogeneity of surface polymerization heterogeneity.[51] Finally, at a yet higher brush density, S4, repulsion is felt on approach at ~25 nm due to the strong chain extension associated with a chain separation of $0.7R_g$. No adsorption can take place in this tightly packed environment, and the retraction curve is identical to the approach curve with no evidence of attraction. Hence, all three measurements give a consistent estimate of chain extension, albeit from different features of the force−distance curves.

The other feature of these AFM studies that varies in a regular way with chain density is the average magnitude of the attraction reported by the tip on retraction for the various surfaces probed. Figures 4B and 5A−C demonstrate that the mean attractive force decreases from the relatively strong short-range hydrophobic interaction between the tip and the hydrophobic initiator-coated surface (Figure 4B) and then decreases as the chains density increases. The decrease represents the difference between the magnitudes of the stronger hydrophobic force and the weaker force produced by the steric force as the chain density is increased. The force histograms suggest that fewer and fewer hydrophobic events contribute to the force distributions as the polymer adsorption forces begin to dominate with increasing chain density as evidenced by the separations at which attraction is present. The densest brush illustrated in Figure 5C (0.22 chains/nm^2) causes a very weak average adhesion (0.027 ± 0.053 nN), which suggests that the contributions from F_H are almost completely counterbalanced by the repulsive force exerted by the dense brush structure. At this chain density, with a value of $D/R_g = 0.71$, the barrier protecting the underlying hydrophobic surface from the AFM tip was complete. Increasing the graft density further (S5, chain density = 0.31 chains/nm^2; $D/R_g = 0.51$) produced a stronger repulsion with overlapping approach and retraction traces in all cases, consistent with the presence of a well-established steric barrier.

3.5.2. Effect of Graft Density on the Barrier Capacity of Partially Cleaved PDMDOMA-diol (28%) Brushes Whose Hydrophilicity Has Been Chemically Manipulated. In these experiments a change in the hydrophobic/hydrophilic character of the grafted brush layer was achieved by partial hydrolysis of the dioxolane side chain. For high graft densities AFM force curves did not distinguish the differences in hydrophilicity; i.e., S4-diol (28%; data not shown) curves were similar to those for S4-diol (100%, Figure 5C). The GPC analysis shown in Figure 2 indicated a relatively lower hydrophilicity for S4-diol (28%) compared to S4-diol (100%), however. Water contact angle data to be discussed below likewise detected differences in hydrophilicity between these two brushes. The relative insensitivity of AFM is possibly due to the current experimental setup which was not optimized to detect such small differences. Since this repulsion is largely based on changes in the chain entropy, it is perhaps not surprising that the chemical nature of the hydrated brushes, which would be expected to dominate enthalpic interactions, did not play a noticeable role in these measurements. In contrast, at lower graft densities (0.04−0.12 chains/nm^2), slight but consistent differences were observed between two types of samples (Figure 6). Since, as we have argued above and elsewhere, the attractions measured at these D/R_g values are determined largely

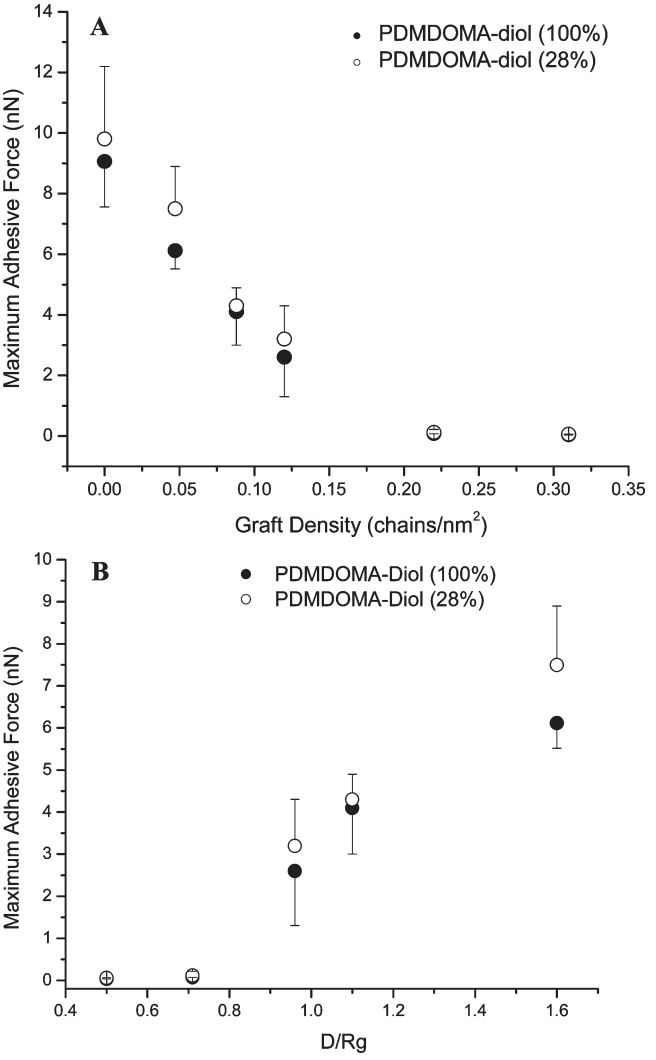

Figure 6. Correlation of the maximum adhesive force (PDMDOMA-diol, 100%, 28%) with (A) graft density and (B) D/R_g. Each data point represents the average of 50 measurements; error bars represent one standard deviation.

by chain adsorption to the AFM tip, which is related to both entropy and enthalpy effects, the chemical nature of the monomer would be expected to play a role. The somewhat stronger adhesion values observed for the 28% diol brushes suggest slightly stronger adsorption between the chains and the hydrophobic surface of the AFM tip, an interaction which is consistent with the more hydrophobic nature of these polymers compared to the 100% diol brushes. We believe the fact that we have, with this one polymer system, been able to examine parameters that capture many of the basic aqueous brush properties implies a wider applicability to the conclusions given above.

3.5.3. Effect of Hydrophilicity, Mediated by Temperature, on the Barrier Capacity of PDMDOMA Brushes

a. Barrier Capacity of a Hydrated PDMDOMA Brush. Like many complex organic monomers containing both hydrophilic and hydrophobic moieties, PDMDOMA in aqueous solution exhibits an LCST at about 23 °C due to the reduction in solubility with increasing temperature associated with weaker H-bonding with water and potentially other changes in enthalpy and entropy.

In this study we chose brush S4 (PDMDOMA, 0.22 chains/nm^2) to investigate the effect of temperature-dependent hydrophilicity on barrier capacity. As discussed above,

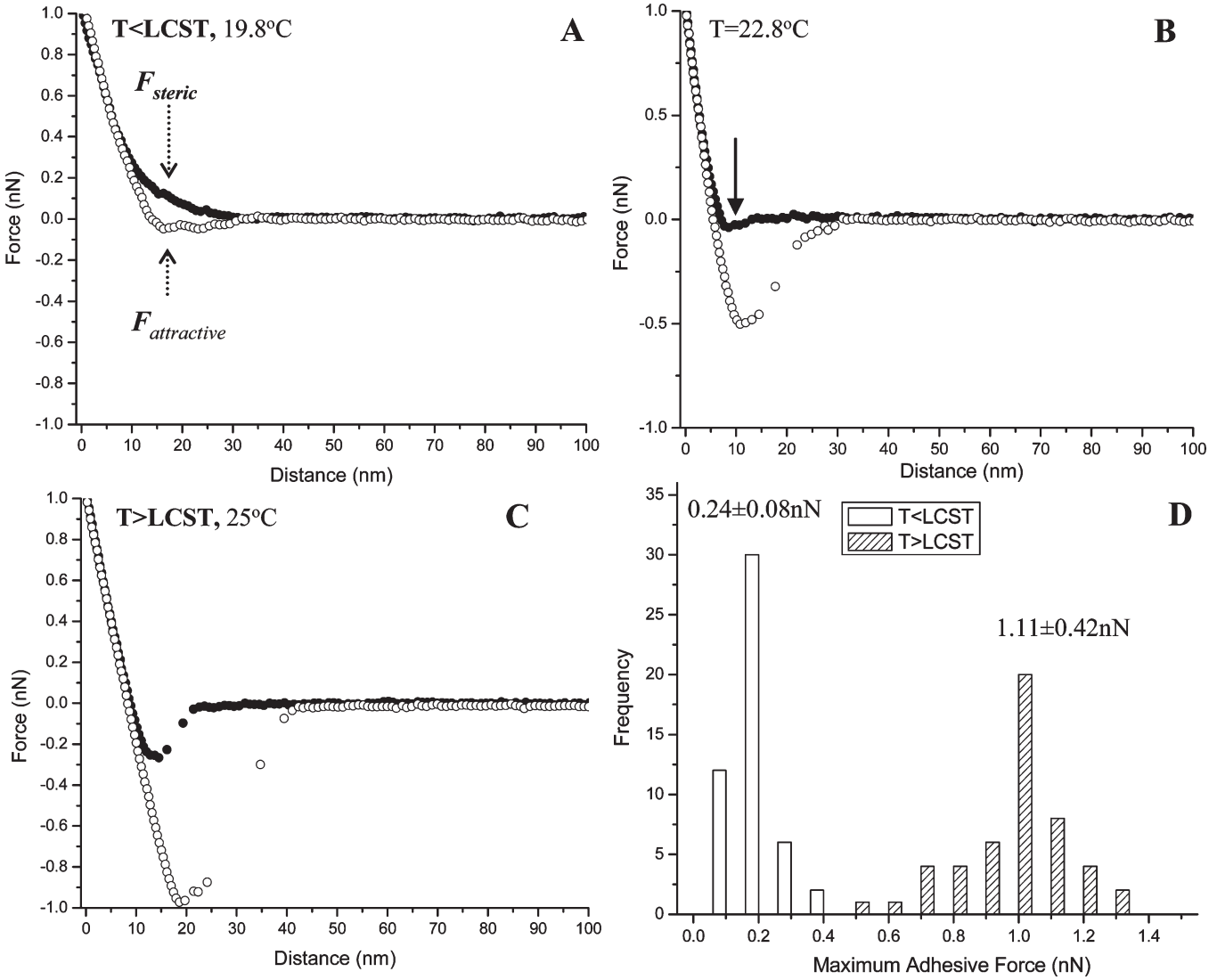

Figure 7. Force measurement of S4 (grafting density = 0.22 chains/nm^2) at variable temperatures. Representative approach (filled circles) and retraction (open circles) force curves are shown. (A) $T <$ LCST, the PDMDOMA brush was in a hydrated state. (B) T 20 °C $< T <$ 23 °C, the brush was in a transitional state. (C) $T >$ LCST, the brush was in a collapsed state. (D) Probability distribution histograms for the maximum adhesive force during retraction when the temperature was lower or higher than the LCST.

the S4-diol (100%) (Figure 5C) showed pure steric repulsion behavior with no hysteresis between the approach and retraction curves and therefore no contribution from either the hydrophobic or chain adsorption sources of attraction. A significant change in the force profile between S4 (PDMDOMA) and S4-diol (PDMDOMA-diol (100%) is observed in Figure 7A compared to 5C, however, even though the PDMDOMA brush is well below the critical temperature. It is seen that although the approach curve in Figure 7A shows pure steric repulsion, the retraction profile shows a small attractive component beyond the range of hydrophobic interactions between the tip and the underlying wafer surface. As noted above, given the location at which this occurs, the weak attraction must be due to polymer adsorbing very weakly to the tip. This interaction was not observed with the 100% diol S4 so it must result from the more hydrophobic nature of the DMDOMA monomer compared to the associated diol. Hence, even in this hydrated form the brush shows some hydrophobic character as it interacts with the AFM tip. Weak attractions of this type have been discussed previously by Goodman et al.[44] and noted by Ishida and collaborators.[50]

As the temperature is increased, the brush begins to retract and collapse due to internal hydrophobic bonding and the attraction between the brush and tip becomes more obvious, appearing in the approach and retraction arms of the cycle (Figure 7B,C). On approach the tip is attracted to the brush by enhanced adsorption associated with the decreased aqueous solubility at higher temperatures at a location interpreted as being near the outer edge of the brush. As the tip continues to be forced into the brush, steric repulsion dominates and strong repulsion is observed. On retraction, because the tip has been inserted deep in the brush much more chain adsorption to the tip can occur and chains are pulled out of their equilibrium configuration by the retracting tip, the more so the stronger the monomer−tip interaction (Figure 7B compared to 7C). The magnitude of the maximum attractive force likewise goes up as the temperature is increased (Figure 7D), consistent with the above picture.

The fully collapsed brush (Figure 7C) forms a hydrophobic surface, but its character is clearly different from the initiator-coated surface probed in Figure 4A. The mean attraction is much higher in the former case (Figure 4B),

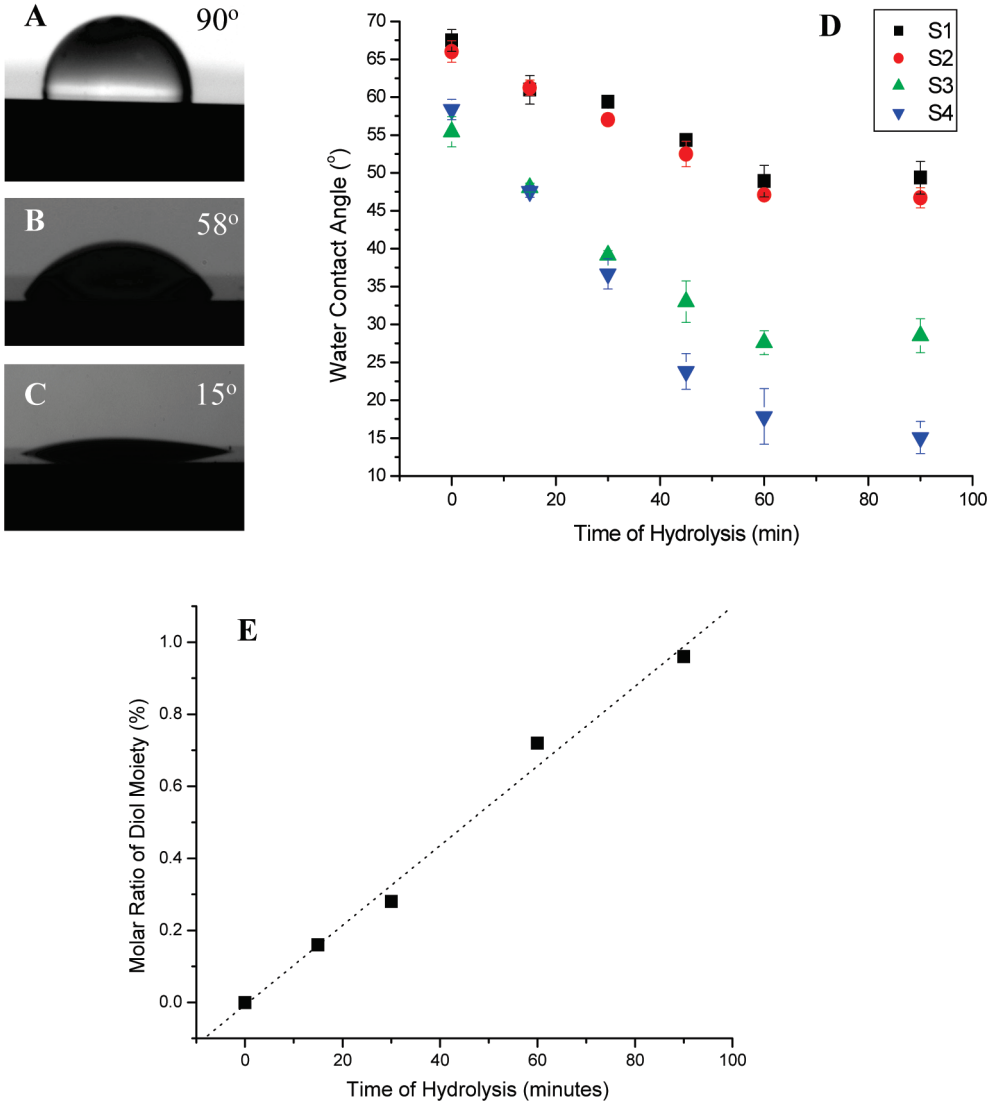

Figure 8. (A) Water contact angle pictures of ATRP-initiator deposited wafer surface, (B) PDMDOMA (S4), and (C) PDMDOMA-diol (100%, S4). (D) Relationship of water contact angle of S1 to S4 with time of hydrolysis. Contact angle was measured at 25 °C. (E) Relationship between the molar content of diols in the PDMDOMA solution polymer and hydrolysis time (hydrolysis was conducted in 10% HAc at 45 °C).

and the tip jumps to contact whereas the attraction develops over a greater distance (Figure 7C) as the polymer chains interact with the tip. The repulsion once the tip has contacted the edge of the hydrophobic region increases with a much lower slope in the polymer case as well, due to the softer nature of the polymer layer.

3.6. Correlation of Barrier Capacity and Water Contact Angle with the Polymer Brush-Coated Surface. To support the results obtained from the AFM force measurements, we measured the static contact angle of water drops at 25 °C on the various brush preparations as a way to compare their relative hydrophobicities. An image of a water droplet on the initiator-coated wafer surface is shown in Figure 8A; the contact angle $>90°$ suggests a relatively high hydrophobicity for this surface. This observation is consistent with the results of the AFM adhesive force measurements in which a strong hydrophobic interaction was observed (Figure 4A,B). The presence of PDMDOMA/PDMDOMA-diol brushes on the silicon wafers led to a decrease in the water contact angle. Figure 9 illustrates the effect of graft density on water contact angle of three different PDMDOMA brushes. For collapsed PDMDOMA brushes, the water contact angle was 67.5°, 66.1°, 55.4°, and 58.5° when graft density was 0.044, 0.089, 0.12, and 0.22 chains/nm^2, respectively. Although this change was significant, based on the small error bars recorded, the change in contact angle was limited. Evidently in the collapsed state the hydrophobicity was relatively insensitive to the graft density. In contrast, the contact angle of PDMDOMA-diol (28%) and PDMDOMA-diol (100%) showed a more pronounced dependence on graft density as it was progressively increased. For instance, at graft densities 0.044, 0.089, 0.12, and 0.22 chains/nm^2, the water contact angle of PDMDOMA-diol (100%) was 49.36°, 46.7°, 28.5°, and 15.1°, respectively. A similar result was observed for PDMDOMA-diol (28%). A sharp change in contact angle was observed when the graft density was increased from 0.089 to 0.12 chains/nm^2. This observation paralleled to some degree the AFM force measurements (Figure 6A) which showed the attractive force approaching zero in this range.

To study the effect of hydroxyl content (hydrophilicity) on surface wettability, variations in the degree of hydrolysis of PDMDOMA brushes were used. Surface hydrophilicity gradually increased as diol content increased (Figure 8D). The extent of hydrolysis was estimated from the hydrolysis of PDMDOMA performed in solution under the same hydrolytic conditions (Figure 8E). Since the hydrolyzing

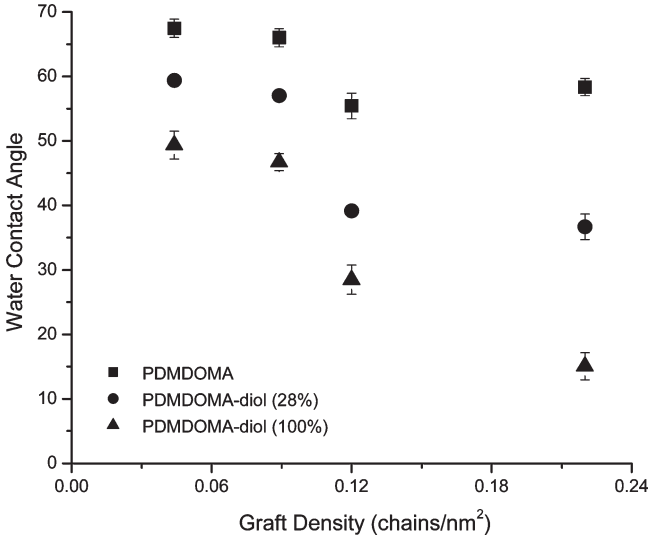

Figure 9. Evolution of water contact angle with increased graft density for PDMDOMA brushes with different hydrophilicity.

agent, acetic acid, is small, its diffusion into PDMDOMA brush should not be greatly limited by size effects. In addition, since acetic acid is a good solvent for PDMDOMA, no exclusion due to incompatibility would be expected, suggesting acetic acid should have full access to the grafted chains. Therefore, we believe the hydrolysis rate and extent for the brushes should resemble those for solution polymer. In solution, diol content increased linearly with prolonged hydrolysis time and reached 100% after 90 min (Figure 8E). The water contact angles of S1 to S4-diol (100%) were 49.4°, 46.7°, 28.5°, and 15.1°, respectively (Figure 8D), after 90 min hydrolysis. These values are 26%, 29%, 49%, and 73.7% lower than the corresponding PDMDOMA counterparts (collapsed). The water contact angle results shown in Figure 8D decrease with time as anticipated and correlate well with the hydrolysis rate for solution polymer for the first hour, after which the angle is largely insensitive to prolonged hydrolysis time. This is not surprising given the strong dependence of contact angle on the most external chemical groups on a surface.[52] Hydrolysis deeper in the brush would therefore be expected to have a smaller statistical effect on contact angle, consistent with our observations. Since there is too little polymer on the surface to be released and analyzed in solution, we have made the reasonable assumption that hydrolysis of solution polymer provides a good guide to results for grafted polymer.

Interestingly, although the AFM results did not show significant differences between partially cleaved PDMDOMA (S4-diol, 28%) and completely cleaved brushes (S4-diol, 100%) at high graft density (Figure 6), water contact angles of the two types of brushes exhibited significant differences (Figure 8D). The differences between the AFM and water contact angle results were likely due to the AFM setup for the current study not being optimized to detect small differences between two samples. The contact angle measurement also sampled a much larger surface area carrying many more chains, making small differences easier to detect.

4. Conclusion

We have studied the properties of a novel class of polymer brushes grown from silicon wafers that are capable of preventing hydrophobic interactions with the underlying surface, as reported by AFM, under delineated conditions of graft density and hydrophilicity. A physical model detailing three interactions—a hydrophobic attractive force between the AFM tip and the surface of the wafer carrying ATRP initiators, a steric repulsive force due to the tip constraining the available conformations of the polymer brush chains, and an attractive force between the AFM tip and adsorbing polymer chains—was proposed. The evolution of these interactions after grafting PDMDOMA brushes with different graft densities and hydrophilicities was tracked by AFM. The grafting of PDMDOMA brushes effectively prevented the hydrophobic interactions by the steric effect offered by polymer brushes. Graft density and hydrophilicity of PDMDOMA brushes play important roles in controlling the barrier capacity of these polymer brushes. In general, increases in graft density and hydrophilicity led to higher barrier capacities. Correlations between barrier capacities of PDMDOMA/PDMDOMA-diol brushes with the interfacial properties of surfaces were established by tuning the hydrophilicity and graft density of the polymer brushes. Compared to the pronounced effect exerted by graft density, tuning hydrophilicity has only a limited impact on hydrophobic interactions. The polymer system described here provides a rich set of properties with which to study interfacial properties of aqueous polymer brushes.

Acknowledgment. Financial support from Canadian Institutes of Health Research (CIHR), Canadian Blood Services (CBS), Canada Foundation for Innovation (CFI), the Natural Sciences and Engineering Council, and the Michael Smith Foundation for Health Research (MSFHR) is gratefully acknowledged. The authors thank the LMB Macromolecular Hub at the UBC Center for Blood Research for the use of their research facilities. These facilities are supported in part by grants from the Canada Foundation for Innovation and the Michael Smith Foundation for Health Research. J.N.K. is the recipient of CBS/CIHR new investigator award in transfusion science.

Supporting Information Available: Figures showing effect of different approach speed on rupture forces of S4-PDMDOMA (1S), force−distance profiles of ATRP initiator-modified wafer surface (2S), ^{1}H NMR of PDMDOMA, PDMDOMA-diol (30%), and PDMDOMA-diol (100%) in D_2O (3S), and AFM analysis of contour length of polymer chains on S4-PDMDOMA (4S). This material is available free of charge via the Internet at http://pubs.acs.org.

References and Notes

(1) Williams, D. F. *Biomaterials* **2008**, *29*, 2941–53.
(2) Gorbet, M. B.; Sefton, M. V. *Biomaterials* **2004**, *25*, 5681–03.
(3) Lamba, N. M. K.; Courtney, J. M.; Gaylor, J. D. S.; Lowe, G. D. O. *Biomaterials* **2000**, *21*, 89–96.
(4) Lappegard, K. T.; Riesenfeld, J.; Brekke, O. L.; Bergseth, G.; Lambris, J. D.; Mollnes, T. E. *Ann. Thorac. Surg.* **2005**, *79*, 917–23.
(5) Ware, J. A.; Kang, J.; DeCenzo, M. T.; Smith, M.; Watkins, S.; Slayter, H. S.; Saitoh, M. *Blood* **1991**, *78*, 1713–21.
(6) Kainthan, R. K.; Janzen, J.; Kizhakkedathu, J. N.; Devine, D. V.; Brooks, D.E. *Biomaterials* **2008**, *29*, 1693–1704.
(7) Krishnan, A.; Cha, P.; Liu, Y. H.; Allara, D.; Vogler, E. *Biomaterials* **2006**, *27*, 3187–94.
(8) Alarcon, C. H.; Farhan, T.; Osborne, V. L.; Huck, W. T. S.; Alexander, C. *J. Mater. Chem.* **2005**, *15*, 2089–94.
(9) Inglis, W.; Sanders, G. H. W.; Williams, P. M.; Davies, M. C.; Roberts, C. J.; Tendler, S. J. B. *Langmuir* **2001**, *17*, 7402–05.
(10) Herrwerth, S.; Eck, W.; Reinhardt, S.; Grunze, M. *J. Am. Chem. Soc.* **2003**, *125*, 9359–66.
(11) Wang, D. A.; Chen, B. L.; Ji, J.; Feng, L. X. *Bioconjugate Chem.* **2002**, *13*, 792–803.
(12) Coelho, M. A. N.; Vieira, E. P.; Motschmann, H.; Mohwald, H.; Thunemann, A. F. *Langmuir* **2003**, *19*, 7544–50.
(13) Peter, K.; Schwarz, M.; Conradt, C.; Nordt, T.; Moser, M.; Kubler, W.; Bode, C. *Circulation* **1999**, *100*, 1533–9.
(14) Videm, V. *Biomaterials* **2004**, *25*, 43–51.
(15) Weber, N.; Wendel, H. P.; Ziemer, G. *Biomaterials* **2002**, *23*, 429–39.

(16) Kooten, T. G.; Spijker, H. T.; Busscher, H. J. *Biomaterials* **2004**, *25*, 1735–47.
(17) MacDonald, D. E.; Deo, N.; Markovic, B.; Stranick, M.; Somasundaran, P. *Biomaterials* **2002**, *23*, 1269–79.
(18) Bhat, R. R.; Chaney, B. N.; Rowley, J.; Vinson, A. L.; Genzer, J. *Adv. Mater.* **2005**, *17*, 2802–07.
(19) Mei, Y.; Wu, T.; Xu, C.; Langenbach, K. J.; Elliott, J. T.; Vogt, B. D.; Beers, K. L.; Amis, E. J.; Washburn, N. R. *Langmuir* **2005**, *21*, 12309–14.
(20) Feng, W.; Brash, J. L.; Zhu, S. *Biomaterials* **2006**, *27*, 847–55.
(21) Unsworth, L. D.; Sheardown, H.; Brash, J. L. *Langmuir* **2005**, *21*, 1036–41.
(22) Ostuni, E.; Chapman, R. G.; Holmlin, R. E.; Takayama, S.; Whitesides, G. M. *Langmuir* **2001**, *17*, 5605–20.
(23) Singh, N.; Cui, X.; Boland, T.; Husson, S. M. *Biomaterials* **2007**, *28*, 763–71.
(24) Kizhakkedathu, J. N.; Janzen, J.; Le, Y.; Kainthan, R. K.; Brooks, D. E. *Langmuir* **2009**, *25*, 3794–801.
(25) Yeh, P. Y. J.; Kainthan, R. K.; Zou, Y.; Chiao, M.; Kizhakkedathu, J. N. *Langmuir* **2008**, *24*, 4907–16.
(26) Bernards, M. T.; Cheng, G.; Zhang, Z.; Chen, S.; Jiang, S. *Macromolecules* **2008**, *41*, 4216–19.
(27) Ma, H.; Hyun, J.; Stiller, P.; Chilkoti, A. *Adv. Mater.* **2004**, *16*, 338–341.
(28) Ladd, J.; Zhang, Z.; Chen, S.; Hower, J. C.; Jiang, S. *Biomacromolecules* **2008**, *9*, 1357–61.
(29) (a) Arieh, B. N. *Hydrophobic Interaction*; Plenum Press: New York, 1980. (b) Chandler, D. Nature (London) 2005, 437, 640–47. (c) Meyer, E. E.; Rosenberg, K. J.; Israelachvili, J. N. Proc. Natl. Acad. Sci. U.S.A. 2006, 103, 15739–746.
(30) Reid, D. S.; Quickenden, M. A. J.; Franks, F. *Nature (London)* **1969**, *224*, 1293–94.
(31) Geisler, M.; Pirzer, T.; Ackerschott, C.; Lud, S.; Garrido, J.; Scheibel, T.; Hugel, T. *Langmuir* **2008**, *24*, 1350–55.
(32) (a) Yamamoto, S.; Ejaz, M.; Tsujii, Y.; Fukuda, T. *Macromolecules* **2000**, *33*, 5608–12. (b) Husseman, M.; Malmstrom, E. E.; McNamara, M.; Mate, M.; Mecerreyes, D.; Benoit, D. G.; Hedrick, J. L.; Mansky, P.; Huang, E.; Russel, T. P.; Hawker, C. J. *Macromolecules* **1999**, *32*, 1424–31.
(33) Goodman, D.; Kizhakkedathu, J. N.; Brooks, D. E. *Langmuir* **2004**, *20*, 3297–3303.
(34) Matyjaszewski, K.; Miller, P. J.; Shukla, N.; Immaraporn, B.; Gelman, A.; Luokala, B. B.; Siclovan, T. M.; Kickelbick, G.; Vallant, T.; Hoffmann, H.; Pakula, T. *Macromolecules* **1999**, *32*, 8716–24.
(35) Zou, Y.; Brooks, D. E.; Kizhakkedathu, J. N. *Macromolecules* **2008**, *41*, 5393–5405.
(36) Manuscript in preparation.
(37) Florin, E. L.; Rief, M.; Lehmann, H.; Ludwig, M.; Dornmair, C.; Moy, V. T.; Gaub, H. E. *Biosens. Bioelectron.* **1995**, *10*, 895–901.
(38) Wang, M.; Cao, Y.; Li, H. B. *Polymer* **2006**, *47*, 2548–54.
(39) Ducker, W. A.; Sendan, T. J.; Pashley, R. M. *Langmuir* **1992**, *8*, 1831–6.
(40) Wu, T.; Efimenko, K.; Vlcek, P.; Suber, V.; Genzer, J. *Macromolecules* **2003**, *36*, 2448–53.
(41) Dimitrov, I.; Trzebicka, B.; Muller, A. H. E.; Dworak, A.; Tsvetanov, C. B. *Prog. Polym. Sci.* **2007**, *32*, 1275–343.
(42) Luzinov, I.; Minko, S.; Tsukruk, V. V. *Prog. Polym. Sci.* **2004**, *29*, 635–98.
(43) Plunkett, K. N.; Zhu, X.; Moore, J. S.; Leckband, D. E. *Langmuir* **2006**, *22*, 4259–66.
(44) Goodman, D.; Kizhakkedathu, J. N.; Brooks, D. E. *Langmuir* **2004**, *20*, 2333–40.
(45) Sonnenberg, L.; Parvole, J.; Kühner, F.; Billon, L.; Gaub, H. E. *Langmuir* **2007**, *23*, 6660–66.
(46) Yamamoto, S.; Tsujii, Y.; Fukuda, T. *Macromolecules* **2000**, *33*, 5995–98.
(47) Cuenot, S.; Gabriel, S.; Jerome, R.; Jerome, C.; Fustin, C. A.; Jonas, A.; Duwez, A. S. *Macromolecules* **2006**, *39*, 8428–33.
(48) Goodman, D.; Kizhakkedathu, J. N.; Brooks, D. E. *Langmuir* **2004**, *20*, 6238–45.
(49) Jones, D. M.; Smith, J. R.; Huck, W. T. S.; Alexander, C. *Adv. Mater.* **2002**, *14*, 1130–34.
(50) Ishida, N.; Kobayashi, M. *J. Colloid Interface Sci.* **2006**, *297*, 513–19.
(51) Zou, Y.; Kizhakkedathu, J. N.; Brooks, D. E. *Macromolecules* **2009**, *42*, 3258–68.
(52) Jisr, R. M.; Rmaile, H. H.; Schlenoff, J. B. *Angew. Chem., Int. Ed.* **2005**, *44*, 782–5.
(53) (a) Alexander, S. *J. Phys. (Paris)* **1977**, *38*, 983. (b) de Gennes, P. G. *Macromolecules* **1980**, *13*, 1069–75. (c) Milner, S. T. *Science* **1991**, *251*, 905–14.